Anal. Chem. **2002,** *74,* 1249−1255

Examination of Theoretical Models in External Voltage Control of Capillary Electrophoresis

Nanette K. Hartley and Mark A. Hayes*

Department of Chemistry and Biochemistry and The Center for Solid State Electronics Research, Arizona State University, Tempe, Arizona 85287-1604

Control of electroosmosis by an external voltage in capillaries of varying geometry was examined and investigated. Controlled geometric factors included inner and outer radii, external electrode coverage area, and the method of voltage application. The behavior of the flow in response to the external voltage from earlier work and this study were compared to existing literature models. A noticeable lack of correlation between the current modeling theories and the published data is noted. In light of these results, suggestions for further areas of investigation of a description of external voltage flow control mechanism are suggested.

Capillary electrophoresis (CE) has proven to be an exceptionally useful technique for highly efficient separations and the identification of molecules based on elution time.[1,2] The technique is, however, plagued by variations in retention time due to solute and wall interactions,[3−5] which directly affect the flow rate of the system. Several methods have been used to address the variability arising from this type of interaction: buffer additives,[6−10] buffer concentration,[11−13] buffer pH,[11,14,15] and wall coatings.[6,7,16] These methods, although addressing the initial state of the system, are not responsive to alterations that occur during processing. A more powerful approach to controlling flow rate is a dynamic method whereby the rate can be directly altered in response to transient variations.

Dynamic control of flow rate may be achieved with the use of external voltages (assuming that it is coupled with a flow monitoring method);[17,18] however, the reliable use of external voltage control (EVC) requires that the phenomena be thoroughly understood and well-characterized. A number of methods have been used to apply EVC under several sets of system conditions (magnitude of axial voltage field, buffer properties, surface treatments, etc.), and these resulted in a large range of control efficiencies and several methods of examining the results.[17−27] The underlying mechanism of control is also still being discussed in the literature.[17,28,29]

EVC has been described by two theories: the electrostatic-based model, first put forward in separate, but related works by the research groups of Lee[17] and Ewing;[18] and the Gaussian-based model described by Poppe et al.[28] The electrostatic-based theory includes a cylindrical capacitor model that describes the additional surface charge generated by an external voltage (EV) as

$$\sigma_T = \frac{\epsilon_Q \epsilon_0 V_r}{r_i \ln(r_0/r_i)} \quad (1)$$

where σ_T is the theoretical surface charge density due to the EV, ϵ_Q is the dielectric constant of the wall material, ϵ_0 is the permittivity of free space, V_r is the applied voltage, and r_i and r_o

* To whom correspondence should be addressed. E-mail: mhayes@asu.edu.

(1) Li, S. F. Y. *Capillary Electrophoresis*; Elsevier: Amsterdam, New York, 1992.
(2) Camilleri, P. *Capillary Electrophoresis*; CRC Press: Boca Raton, Fl, 1998.
(3) Rice, C. L.; Whitehead, R. *J. Phys. Chem.* **1965**, *69*, 4017−4024.
(4) Overbeek, J. T. G. In *Colloid Science*; Kruyt, Ed.; Elsevier: Amsterdam, 1952; Vol. 1, Chapter 5.
(5) Davies, J. T.; Rideal, E. K. *Interfacial Phenomena*, 2nd ed.; Academic Press: New York, 1963.
(6) Jorgenson, J. W.; Lukacs, K. D. *Science* **1983**, *222*, 266−272.
(7) Hjerten, S. *J. Chromatogr.* **1985**, *347*, 191−198.
(8) Bruin, G. J. M.; Chang, J. P.; Kuhlman, R. H.; Zegers, K.; Kraak, J. C.; Poppe, H. *J. Chromatogr.* **1989**, *471*, 429−436.
(9) VanOrman, B. B.; Liversidge, G. G.; McIntire, G. L.; Olefirowics, T. M.; Ewing, A. G. *J. Microcolumn. Sep.* **1990**, *2*, 176−180.
(10) Schwer, C.; Kendler, E. *Anal. Chem.* **1991**, *63*, 1801−1807.
(11) Lukacs, K. D.; Jorgenson, J. W. *J. High Resolut. Chromatogr., Chromatogr. Commun.* **1985**, *8*, 407−411.
(12) Issaq, H. J.; Atamna, I. Z.; Muscik, G. M.; Janini, G. M. *Chromatographia* **1991**, *32*, 155−161.
(13) Atamna, I. Z.; Metral, C. J.; Muschik, G. M.; Issaq, H. J. *J. Liq. Chromatogr.* **1990**, *13*, 3201−3216.
(14) Lambert, W. J.; Midddleton, D. L. *Anal. Chem.* **1990**, *62*, 1585−1587.
(15) McCormick, R. M. *Anal. Chem.* **1988**, *50*, 2322−2328.
(16) Moseley, M. A.; Deterding, L. J.; Tomer, K. B.; Jorgenson, J. W. *Anal. Chem.* **1991**, *63*, 109−114.
(17) Lee, C. S.; Wu, C.-T.; Lopes, T.; Patel, B. *J. Chromatogr.* **1991**, *559*, 133−140.
(18) Hayes, M. A.; Kheterpal, I.; Ewing, A. G. *Anal. Chem.* **1993**, *65*, 27−31.
(19) Wu, C.-T.; Lopes, T.; Patel, B.; Lee, C. S. *Anal. Chem.* **1992**, *64*, 886−891.
(20) Keely, C. A.; Holloway, R. R.; van de Goor, T. A. A. M.; McManigill, D. *J. Chromaogr. A* **1993**, *652*, 283−289.
(21) Culbertson, C. T.; Jorgenson, J. W. *J. Microcolumn Sep.* **1999**, *11*, 167−174.
(22) Tsai, P.; Patel, B.; Lee, C. S. *Anal. Chem.* **1993**, *65*, 1439−1442.
(23) Kasicka, V.; Prusik, Z.; Sazelova, P.; Barth, T.; Brynda, E.; Machova, L. *J. Chromatogr. A* **1997**, *772*, 221−230.
(24) Bello, M. S.; Capelli, L.; Righetti, P. G. *J. Chromatogr. A* **1994**, *684*, 311−322.
(25) Wu, C.-T.; Huang, T.-L.; Lee, C. S. *Anal. Chem.* **1993**, *65*, 568−571.
(26) Wu, C.-T.; Lee, C. S.; Miller, C. J. *Anal. Chem.* **1992**, *64*, 2310−2311.
(27) Huang, T.-L.; Tsai, P.; Wu, C.-T.; Lee, C. S. *Anal. Chem.* **1993**, *65*, 2887−2893.
(28) Poppe, H.; Cifuentes, A.; Kok, W. T. *Anal. Chem.* **1996**, *68*, 888−893.
(29) Bard, A. J.; Faulkner, L. R. *Electrochemical Methods*; John Wiley & Sons: New York, 1980.

10.1021/ac010816y CCC: $22.00
Published on Web 02/08/2002

are the inner and outer capillary radii, respectively.[18] Flow rate in CE is related to the potential drop across the diffuse layer, ζ, which is influenced by the surface charge density at the inner wall of the capillary.[29] This results in a change in flow rate with a change in surface charge density arising from the EV. According to eq 1, the largest change in flow rate for the same applied voltage is predicted to occur in small internal diameter and thin-walled systems. Later works have used this model without further examination.

External voltage flow control has recently been extended to microfluidic devices.[30,31] A much larger range of geometric configurations are available in this format, both from the additional structural support provided by the substrate and the high-resolution fabrication techniques. Schasfoort et al.[30] has constructed a chip with 390-nm-thick walls and shows measurable flow control with the application of only ~100 V. Polson and Hayes[31] have shown flow rate changes in a 50-μm wall system with the application of 120 V. This result is a significant departure from both previous experimental results and theoretical predictions from either existing model. It is unclear how the device of Polson and Hayes achieved such results, since the wall thickness differs little from fused-silica capillary systems.

A variety of issues have prompted this study: Variations may occur in flow control efficiencies in standard fused-silica capillaries, the ongoing discussions about the underlying mechanism of EVC, and the disparate geometries beginning to appear in microdevices, with some producing unusual results. The effects of capillary dimensions on flow control were investigated by both performing experiments with a variety of inner and outer diameter capillaries and reevaluating relevant experimental results from the literature. Both the new data and the literature values were evaluated against two theoretical models: the electrostatic-based description of EVC[17,18] and the Gaussian description proposed by Poppe, Cifuentes, and Kok.[28] Capillaries of inner diameters (i.d.) of 6−75 μm and outer diameters (o.d.) of 150 or 360 μm were used, and the external voltage was varied from −25 to +25 kV in 5-kV increments. This work was compared with all literature work with similar buffer pH, concentration, and composition.

THEORY

Current EVC literature describes two different modeling regimes for this phenomenon. Initial modeling describes this phenomenon in terms of simple electrostatics and geometry, whereby the capillary acts as a cylindrical capacitor, building up charge from the EVC.[29] The core capacitive nature of this approach is described in Equation 1. This model applies the standard electric double layer theory (either straight Gouy−Chapman or with the Stern modification) with the limitations imposed by the Debye−Hückel approximations. For purposes of this discussion, this approach will be identified as the electrostatic model.

Alternatively, Poppe, Cifuentes, and Kok[28] described the EVC effect using a Gaussian model. In this theory, the effect of the EVC is shown by

$$\phi^{G}(x) = \frac{2kT}{ze} \ln \frac{[S + (S^2 + 1)^{1/2} + 1][1 + \exp(-\kappa x)] - 2\exp(-\kappa x)}{[S + (S^2 + 1)^{1/2} + 1][1 - \exp(-\kappa x)] + 2\exp(-\kappa x)} \quad (2)$$

where the reference defines the variable as follows: $\phi^{G}(x)$ is the Gaussian ζ potential, k is the Boltzmann's constant, T is the temperature, z is the charge on the electrolyte ion, e is the elementary charge, x is the distance into the diffuse layer, and κ is the inverse diffuse layer thickness, defined by

$$\kappa = \left(\frac{2n^0 z^2 e^2}{\epsilon_{aq}\epsilon_0 kT}\right)^{1/2} \quad (3)$$

with n^0 being the number concentration of the electrolyte, ϵ_{aq} is the dielectric constant of the buffer, and all other variables as described above, and S being a parameter defined by

$$S = \frac{\sigma_d}{(8kT\epsilon_{aq}\epsilon_0 n^0)^{1/2}} \quad (4)$$

where σ_d is the total surface charge density of the diffuse layer in solution, regardless of its source. In this model, arbitrary magnitudes for variables are used to adjust the outcome to match experimental data. For instance, δ, which is listed as the proposed stagnant layer thickness of the outer Helmholtz plane, is set at x = 0.8 nm; κ (the inverse diffuse layer thickness) is fixed at 1.36 nm for all systems without justification; the ionic strength is used as a fitting factor to adjust the model to the initial flow rate; and all experimental data presented were corrected with a linear percent coverage factor (see below for discussion of validity of this correction factor). For purposes of this discussion, the model of Poppe, Cifuentes, and Kok will be identified as the Gaussian model, and all of the values used here are those cited in the source work.[28]

Experimental Graph. In this work, categories of method of EVC application were assigned for data analysis. The data used in each category are as follows: resistive sheath (refs 18, 22), concentric capillary (refs 26−29), conductive sheath (refs 18, 19−21, 29), ionized air (ref 17), and parallel plate (experimental data). The comparison of disparate data from within this study and from the literature sources (varying inner and outer diameters, voltage ranges, magnitudes) requires that mathematical manipulations be used to generate a meaningful visual relationship. The underlying assumptions to these manipulations are 2-fold: first, that the capillary is acting as a cylindrical capacitor and that standard electric double-layer phenomena are occurring at the inner wall solid−solution interface. Secondarily, in light of the nonlinearity of the relationship, only the total range of change, both in terms of external potential range and change of electroosmotic mobility coefficient, is plotted, thus avoiding some of the ambiguity and the subtlety of the nonlinear relationship between the applied external voltage and the electroosmotic flow rate. The change in EOF is calculated as the coefficient at the most positive voltage

(30) Schasfoort, R. B. M.; Schlautmann, S.; Hendrikse, J.; van den Berg, A. *Science* **1999**, *286*, 942−945.
(31) Polson, N. A.; Hayes, M. A. *Anal. Chem.* **2000**, *72*, 1088−1092.

used minus the coefficient at the most negative voltage used. Surface charge plots are generated in the following manner: a theoretical surface charge is calculated based on the cylindrical capacitor model using eq 1. This value is then plotted against the surface charge of the capillary calculated from the experimental data, in essence, plotting the theoretical surface charge vs the experimental surface charge. To calculate the capillary surface charge for the capacitive model, σ_C, the observed flow rate is used to calculate the ζ potential within the capillary, according to[18]

$$\zeta = \frac{v_{eof}\eta}{\epsilon_{aq}\epsilon_0 E_{app}} \quad (5)$$

where v_{eof} is the electroosmotic flow velocity, η is the viscosity of the solution, and E_{app} is the applied potential. Next, the potential drop across the double layer (ϕ_0^C) is calculated from[18]

$$\phi_0^C = \frac{\zeta}{\exp(-\kappa\chi)} \quad (6)$$

with χ as the counterion radius and assuming charge neutrality across the double layer/wall system. This information can be used to calculate the surface charge according to[29]

$$\sigma_C = (8kT\epsilon_{aq}\epsilon_0 n^0)^{0.5} \sinh\left(\frac{ze\phi_0^C}{2kT}\right) \quad (7)$$

The calculated surface charge (σ_C) is plotted as a function of the theoretical surface charge (σ_T).

EXPERIMENTAL SECTION

Chemicals. Buffers were prepared using deionized ultralow organic content NANOpure UV (Barnstead, Dubuque, IA) reagent grade water and sodium dihydrogen phosphate (reagent grade, Aldrich Chemical, Milwaukee, WI) with sufficient phosphate added for a concentration of 25 mM, adjusted to pH 3 with 1.0 M NaOH, and brought to final volume. Rhodamine 1,2,3 was obtained from Molecular Probes (Eugene, OR) and used in either 1.6 M (for less than 20-μm i.d. capillaries) or 2×10^{-4} M concentration. Buffers were made with 10% ethanol to ensure solubility of rhodamine samples, degassed with nitrogen filtered through a Drierite gas purifier (W. A. Hammond Drierite, Xenia, OH), sonicated, and then double-filtered (0.5-μm filter unit, Millipore, Bedford, MA) prior to use. Dye samples were prepared by dissolving rhodamine in 2.5 mL of ethanol and diluting to final volume with the running buffer. Gallium was used to coat the capillary surface (Aldrich Chemical, Milwaukee, WI) in some experiments as noted. This was achieved by heating solid gallium slightly, filling a syringe, and applying a layer of gallium onto the capillary exterior between the external voltage plates. Coating was performed around the entire circumference of the capillary by this method.

Fused-silica capillaries (Polymicro Technologies, INC., Phoenix, AZ) were used with a total length of 100 cm. The distance from the sample vial to the detector was 77 cm. Inner capillary diameters of 6, 20, 50, and 75 μm with a 360-μm outer diameter, and 20-, 25-, 50-, and 75-μm-i.d. capillaries with a 150-μm outer diameter were used.

Flow rates were determined using the accelerated marker method adapted from Sandoval and Chen.[32] Briefly, rhodamine 1,2,3 is used as the marker, and pressure is injected for 5 s. A 20-kV separation voltage is then applied for 10 min, during which time the external voltage is also applied. A second 5-s injection of rhodamine follows this migration. The capillary contents are then pushed past the detector window using pressure.

Instrumentation. The experimental system is shown in Figure 1A as a schematic representation from the top view. Capillaries and electrodes were held in a Plexiglas box manufactured in-house. The external voltage was applied through the plates, as illustrated, with the separation voltage applied longitudinally to the capillary. Both external and separation voltages were applied using CZE 1000R high-voltage systems (Spellman High Voltage, Hauppauge, NY). Detection was performed using either an FD 500 fluorescence detector (Groton Technology, Concord, MA) using an excitation wavelength of 500 nm and an emission wavelength of 530 nm or an FD 100 fluorescence detector (Groton Technology, Concord, MA) equipped with a 10-nm band-pass excitation filter of 500 nm and a 10-nm band-pass emission filter of 530 nm. The signal was recorded either by a chart recorder (Ross Recorders, Sparks, NV) or by a National Instruments LabView DAQ card (National Instruments, Austin, TX). Data analysis was performed using Excel (Microsoft Crop. Seattle, WA) programs developed in-house.

The external voltage electrode was isolated from the separation electrode by the Plexiglas walls inside the box to prevent arching between the electrodes. The external voltage electrode is a made of two 10-cm aluminum plates, both of which are connected to high voltage, with the capillary positioned between the plates as shown in the side view (Figure 1B). The capillary is in direct contact with the plates, which ensures that the voltage is applied to the capillary wall.

The effective external voltage is used for all figures in the discussion and is calculated as follows. The potential drop along the length of the capillary covered by the EVC plates changes with distance. However, the difference between the values at the potential at the center of the plate is the same magnitude, but different sign, at each end of the EVC region. Because of this, the differences will cancel each other if the value at the center of the plate is used. The voltage that exists at the center of that plate is calculated by dividing the applied voltage by the total length of the capillary and multiplying this result by the distance from the start of the capillary to the center of the plate. The difference between this voltage and the applied external voltage is then the effective external voltage. EOF data is normalized to the observed mobility with no applied external voltage. The change in EOF is calculated as the EOF velocity at the most positive voltage applied minus the EOF velocity at the most negative voltage applied, or the overall change in EOF for the entire range of external voltage values.

All theoretical points were obtained by inputting experimental conditions into a MathCAD program developed in-house. This program outputs the flow rate at each applied external voltage, as predicted by both the Gaussian and electrostatic methods, as

(32) Sandoval, J. E.; Chen, S.-M. *Anal. Chem.* **1996**, *68*, 2771−2775.

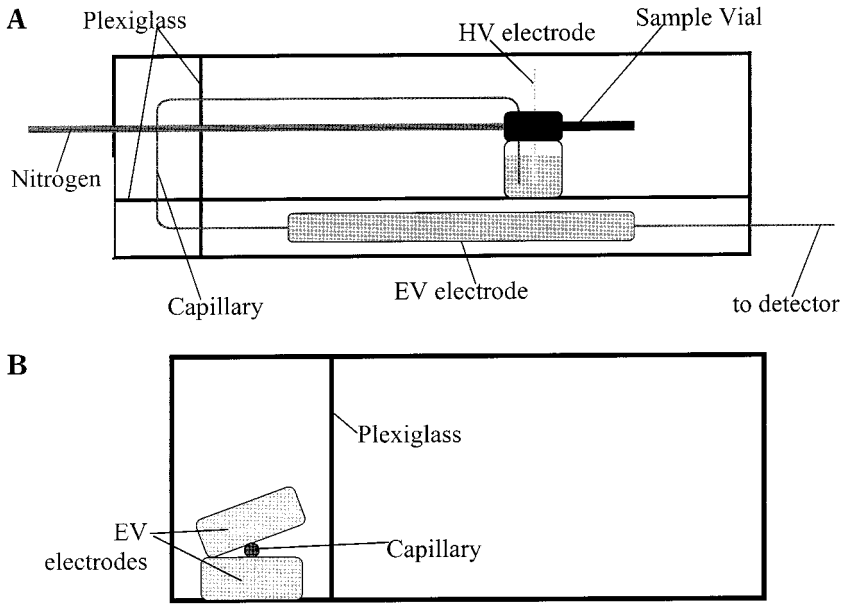

Figure 1. Schematic representation of experimental design (not to scale). Part A is a top view indicating the placement of plexiglass to shield the separation voltage electrode from the external voltage plates. Part B is a side-on view showing the placement of the capillary between the external voltage plates. Both plates are at the same potential. Notice that the capillary circumference is not completely in contact with the plates; the lateral sides of the capillary are not in contact with the electrodes.

described previously. Experimental data were corrected because of less than 100% coverage of the capillary by the EV plates, utilizing the local ζ potential method of Lee et al.[25] or the weighted average method of Chien and Helmer,[33] as discussed in detail later in the text. Corrected experimental data shown in the figures was achieved using the weighted average data.

RESULTS AND DISCUSSION

Recent work has extended external voltage electroosmotic flow control from fused-silica capillaries to microfluidic devices. EVC has proven successful at modifying flow rates in both capillary and microchip formats but with highly varied efficiency. To compare data from disparate devices, system setups, and designs, Polson and Hayes[31] derived an empirical efficiency measurement, Γ, for the EVC effect, given by

$$\Gamma = \frac{\Delta\mu_{eof}}{[V_r/(r_i \ln(r_o/r_i))]} \qquad (8)$$

where all variables used are as previously described. This efficiency factor accounts for the varying capillary geometry and applied field for the comparison of flow rates.

In fused-silica capillaries, on the basis of an assumption of an electrostatic capacitive effect,[18,19,25,33] Γ varied by a factor of 4.[31] The two examples of external voltage flow control on microdevices shows an even greater variance in control efficiency.[30,31] Schasfoort et al. has produced a microdevice with 390-nm-thick walls and has shown an overall change the electroosmotic coefficient of 3.3 $\times$ 10^{-4} cm^2/V s.[30] Polson and Hayes use microchips with 50-μm walls and produce an overall change in the electroosmotic coefficient of 7.9 $\times$ 10^{-5} cm^2/V s.[31] The very thin-walled channel showed an empirical efficiency of about 1.5 times the average conventional capillary experiment, whereas the thicker-walled microdevice demonstrated some 40-times greater efficiency.

Differing Models. Aside from these varied experimental results, the mechanism of the EVC effect is still debated in the literature.[20,28,34] Early work modeled the effect in terms of electrostatic capacitance of the capillary and electric double layer.[17,18,25,33] Somewhat archaic units in this early work were later converted to SI units, thus making them easier to interpret.[20,34] Other later works suggest that a model based on a judiciously chosen set of Gaussian surfaces provides a better description of the experimental data.[28] It has been assumed without thorough investigation that these models describe experimental results; however, the large variations in efficiencies suggests otherwise. Consequently, reasons for the variations were explored in both models to quantitate the variability and fit of the data to the models.

Methods of EVC Application. One possible explanation for the large variation in efficiency for this technique is the method of application for the external potential. It may be instructive to examine plots of the existing models with the experimental data; in that way, the models can be compared quantitatively with the data and with each other (Figures 2 and 3). There appears to be little quantitative difference between the two models in their predictions of EOF for this technique (Figure 2). In the plots (Figure 3), the relationship between the models (electrostatic and Gaussian, only the electrostatic model shown) and the capacitive nature of the system are linear. This assumes a solution pH of 3 and the pK_a for the siloxane surface of 1 $\times$ 10^{-7}. Further modifications to the capacitive nature have been made by Scales et al.[35] and Huang et al.[27] based on the Gouy–Chapman–Stern–

(33) Hayes, M. A.; Kheterpal, I.; Ewing, A. G. *Anal. Chem.* **1993**, *65*, 2010–2013.

(34) Hayes, M. A. *Anal. Chem.* **1999**, *71*, 3793–3798.

(35) Scales, P. J.; Grieser, F.; Healy, T. W.; White, L. R.; Chan, D. Y. C. *Langmuir* **1992**, *8*, 965–974.

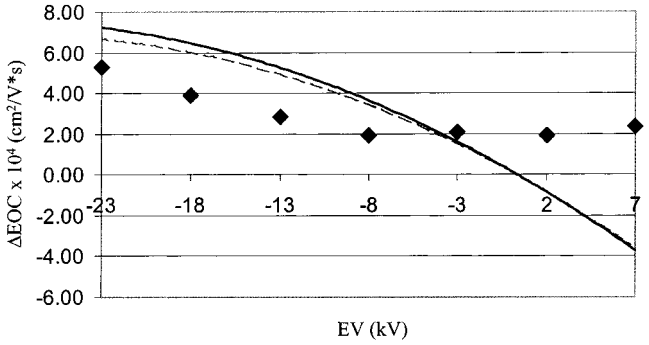

Figure 2. Comparison of theory with experimental data. Symbols: —, electrostatic theory; --, Gaussian theory; ◆, experimental data from a 360-μm-o.d., 6-μm-i.d. capillary. Experimental conditions: 30 kV radial voltage range; 20 kV separation voltage; total capillary length, 1 m; length of radial voltage, 0.175 m; electroosomotic mobility, 2.78 cm^2/V s; counter-ion radius (used in electrostatic calculations), 1.5 $\times$ 10^{-10} m; size of charge layer (used in Gaussian calculations), 8 $\times$ 10^{-10} m. For all data points, $n = 3$. Error bars are included, but are smaller than the points used to represent the data.

Grahme model. Here, the charge density at the edge of the outer Helmholtz plane is given by

$$\sigma_T = \left(\frac{-2\kappa\epsilon_0\epsilon_{aq}kT}{e}\right)\sinh\left(\frac{e\zeta}{2kT}\right) \qquad (9)$$

with all variables being previously defined. Analysis of this modification compared to experimental data provides a theory line that is 2 orders of magnitude higher than the largest flow coefficients seen in the literature data (not shown).

The literature reports the use of a number of methods for EVC application, including ionized air,[26] embedded electrodes on a microchip,[30,31] conductive sheath,[18,20−22,24] resistive sheath,[20] flat conductive plates, and concentric capillary systems.[17,19,25,27] The impact of each of these methods to the overall efficiency can be calculated from the information available from literature sources, although comparing the widely varying physical attributes and experimental conditions of these systems proves to be somewhat cumbersome. To provide relatively simple visual interpretation of these widely varying data, an experimental graph comparing measured surface charge with calculated surface charge densities was generated that assumes electric double layer phenomenon at the inner solid−solution interface and the standard capacitive behavior of the fused-silica capillary (Figure 3). For the conventional capillary approaches, the data can be plotted in five groups: concentric capillaries (▲), ionized air (★), resistive coatings (●), conductive sheaths (×), and flat plate conductors (◆). Upon examination of these experimental plots, maybe somewhat surprisingly, there is little agreement between theory and experiment regardless of the technique of application. Clearly, the few number of data points associated with the ionized air and resistive sheath prevent any meaningful analysis, and although there are enough points for interpretation, the concentric capillaries and conductive sheath data at best only suggest a trend. Since the data for different methods of application lie in different areas, this may suggest that a different mechanism exists for each method; however, not enough data exists to allow a true examination of this question. Although future studies examining the

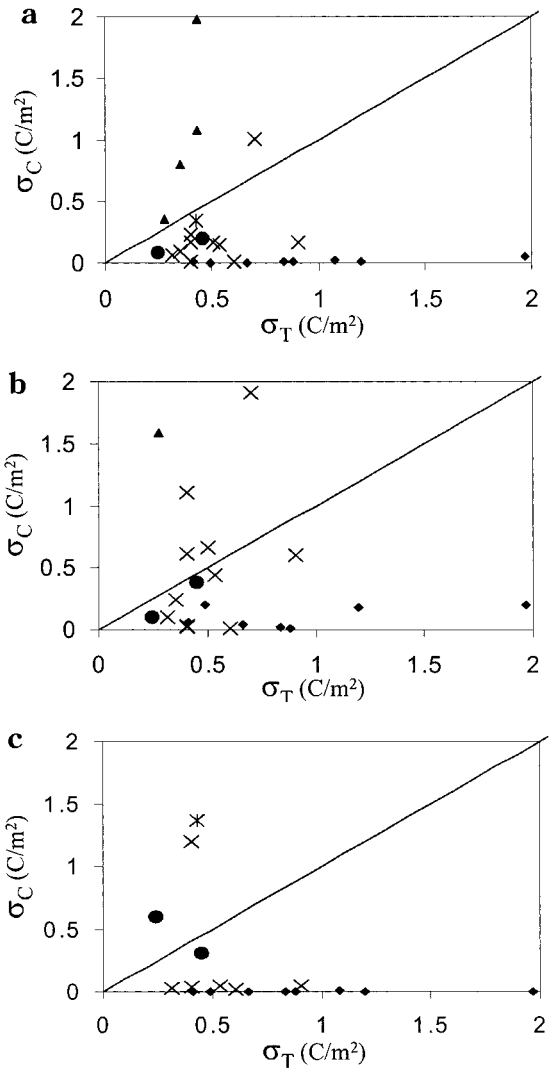

Figure 3. Comparison of literature data with theoretical plots. In all plots, * represents ionized air, × represents the conductive sheath, ▲ represents concentric capillary, ◆ represents the parallel plate, ● represents the resistive sheath, and — represents the theory. Part A represents the comparison of experimental data with theory and correction factors. Part B represents the correction of data for local ζ potential effects. Part C represents the weighted average correction of the experimental data.

technique of application may uncover some identifiable relationships, the data available in the literature do not provide significant insight toward the source of variation in the efficiency of EVC. Use of each method under the same experimental conditions (samples, buffers, pH, etc.) could potentially provide more reliable information into this possibility. Given the wide spread of these data, it is not clear if the basic assumptions in the literature to generate these plots are valid.

Geometric Considerations. Another possible explanation for the changes in efficiency may be due to simple electrostatic geometric considerations; the electrodes (or field exposure for ionized air) used to generate the external fields in standard capillaries cannot cover the entire length of the capillary—the separation and external field electrodes would be too close together, leading to arcing and short circuits. Logic suggests the maximum coverage would be most efficient, and that, in fact, was a working assumption for much of the work in the literature.

However, the literature shows specific data where amount of coverage for the external electrodes varies over a large range, from ~4 to 80%.[33]

Two approaches have been used to examine the effects of the amount of external electrode coverage: one, assuming the completely localized alteration of the ζ potential in portions of the capillary where the electrodes project onto the inner surface; and one, a weighted-average approach in which the electrostatic effects are assumed to influence the entire length of the capillary.

The localized ζ potential approach is the rather simplistic assumption that the field induced by the external electrode influences the surface charge only as it is radially projected into the inner surface of the capillary.[17,28] The concept of localized changes in ζ potential is supported by work from Towns and Regnier.[36] In this work, positively charged proteins were adsorbed to the inner surface of a fused-silica capillary, which induced significant band broadening. This broadening was interpreted to be from flow anomalies generated by electroosmotic forces in the direction opposite to the bulk flow at the sites of adsorption. Similar arguments in agreement with the concept of localized ζ potential changes[37−39] have been shown with the flow imaging studies of Herr et al;[40] however, and in stark contrast, no measurable band broadening has been observed when the external voltage flow control system has been used (although many theoretical discussions have appeared claiming the presence of broadening forces).[17−19,25−27,33,34] Local ζ potential calculations show no improvement in matching data to theory (data not shown), and in fact, remove any suggestion of groupings that were previously evident because of the method of field application. Anderson developed equations for correcting flow based on nonuniform ζ potential using eq 11

$$\zeta = \langle\zeta\rangle\left[1 + 2\cos\left(\frac{\pi z}{L}\right) + 2\sin\left(\frac{\pi z}{L}\right)\right] \qquad (10)$$

where L is the half-length of the capillary, and z is the axial position on the capillary.[43] This would give the ζ potential at a specific place in the capillary. However, this investigation is interested in the mean electroosmotic flow rate, not the rate at a specific point along the capillary. Because of this, it is irrelevant if ζ varies over the capillary length; the mean will reflect the changes in flow rate along the capillary length. Additionally, there is no evidence to suggest that ζ varies over the capillary length. If that were the case, significant band broadening would be observed, and it is not.

Alternatively, the weighted average approach allows for the external electrodes to influence the ζ-potential along the length of the capillary, although the mechanism of this influence has not been established. This, in turn, leads to improved efficiency of control with small amounts of coverage and to a reduced difference in ζ-potential along the length of the capillary and a corresponding reduction in flow anomalies. The weighted average flow regime was first described by Chien and Helmer in association with sample stacking[44] and was applied to EVC by both the Lee and Ewing groups.[25,33] The method provides a correction factor based on the amount of coverage for the capillary by the EV electrodes. The bulk flow is a summation of the larger flow rate in the EVC region, weighted to reflect the percent coverage of the capillary by the EVC electrodes, plus the slower flow rate resulting from the non-EVC region, weighted to the percent coverage of the capillary not covered by the EVC. The correction is based on applying

$$\nu_b = x_s\,\nu_s + (1 - x_s)\,\nu_{us} \qquad (11)$$

where x_s is the portion of the capillary that is covered, ν_{us} is the unsheathed flow velocity, ν_b is the bulk electroosmotic flow, and ν_s is the calculated average flow rate of 100 and 0% coverage used. Again, the data shows a larger spread when corrected in this fashion, with a complete loss of groupings.

The microdevice data and some external electrode configurations provide geometries that are significantly different from a cylindrical system. Microdevice work is accomplished using a parallel plate geometry and, thus, should be described by a flat plate capacitor model. For comparison, the data has been treated as both a cylindrical and a flat plate capacitor. To do this, the cylindrical capacitor factor in eq 1 has been removed and replaced with[45]

$$\sigma = \frac{\epsilon_Q l A}{d} \qquad (12)$$

where l is the length of the EVC plates, A is the projected surface area of the opposing plates of the capacitor, and d is the wall thickness of the channel. A comparison of both electrostatic and Gaussian models with the flat plate capacitor does not yield a better fit of the data to theory (not shown) and is, thus, removed as a potential influencing factor.

In addition, a comparison of flow control with various EVC applications has been completed in this study, in which experiments were performed with the capillary covered in gallium to provide more intimate electrode contact. The purpose of this was to see if greater coverage with conductive material, other than the tangential coverage provided by the plates, would result in better flow control. However, there is no statistical difference between painted and unpainted capillary data, which suggests that the intimacy of contact with the parallel plates is not an issue in the flow rate changes for this system.

Specific Experiments Compared to Theory. Data for a single capillary inner and outer diameter displays good agreement with the models but with the usual deviations for several of the data points (Figure 2). The deviations are generally associated

(36) Towns, J. K.; Regnier, F. E. *Anal. Chem.* **1992**, *64*, 2473.
(37) Bianchi, F.; Chevolot, Y.; Mathieu, H. J.; Girault, H. H. *Anal. Chem.* **2001**, *73*, 3845−3853.
(38) Bianchi, F.; Wagner, F.; Hoffman, P.; Girault, H. H. *Anal. Chem.* **2001**, *73*, 829−836.
(39) Roberts, M. A.; Rossier, J. S.; Bercier, P.; Girault, H. *Anal. Chem.* **1997**, *69*, 2035−2042.
(40) Herr, A. E.; Molho, J. I.; Santiago, J. G.; Mungal, M. G.; Kenny, T. W.; Garguilo, M. G. *Anal. Chem.* **2000**, *72*, 1053−1057.
(41) Potocek, B.; Gas, B.; Kenndler, E.; Stedry, M. *J. Chromatogr. A* **1995**, *709*, 51−62.
(42) Giddings, J. C. *Unified Separation Science*; John Wiley and Sons: New York, 1991.
(43) Anderson, J. L.; Idol, W. K. *Chem. Eng. Commun.* **1985**, *38*, 93−106.
(44) Chien, R.-L.; Helmer, J. C. *Anal. Chem.* **1991**, *63*, 1354−1361.
(45) Serway, R. A. *Physics for Scientists and Engineers*; Saunders Golden Sunburst Series: Philadelphia, 1990.

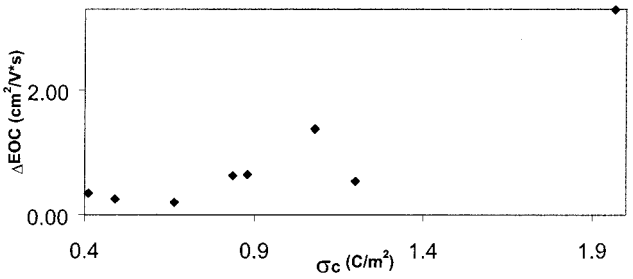

Figure 4. Calculated surface charge plotted against experimental surface charge for varying capillary geometries. Experimental conditions: 30 kV external voltage range; 20 kV separation voltage; total capillary length, 1 m; length of external voltage, 0.175 m. All data points were generated by calculating the surface charge density for the capillary with this external voltage range and plotted against the overall change in EOC for that capillary in this external range.

with the immeasurable factors involved in the solid−solution interface dynamics (limitations in Debye−Huckel assumptions, the magnitude of the variables in the Gaussian model, actual surface pK_a, circular arguments over surface pH compared with solution pH, etc.) and are not the focus of this study. However, taking a variety of capillary inner and outer diameters to form varying capacitance of the capillary system allows for the examination of electrostatic nature of the EVC effect. When the total change in electroosmotic coefficient (EOC) is plotted against the surface capacitance of the capillary (σ_C, Figure 4), there is no convincing relationship between control of EOF and capacitance. This is surprising, because it is expected that as capacitance increases, the change in EOC should also increase. From this perspective, it appears that current modeling does not correlate to the mechanism of EVC. Although many individual experiments in one capillary or with one set of conditions appear to conform to the models, the compiled data does not. Any comparison between systems and conditions does not correlate with the model; the probability that the model describes this system is very low. Because of the lack of correlation, it is important to reexamine our understanding of the mechanism of EVC.

External Voltage Control and Capacitance. The current data suggests that the mechanism of the EVC is not a capacitive effect. Although the mechanism surely is similar to the capacitive model, since single experiments show data within an order of magnitude of the capacitance theory line, no experiment tracks the theoretical line exactly. So where does that leave us? Let us consider the following information.

It is assumed that the charge generated during an external field experiment lies on the interior capillary surface, which has been modeled as the second plate in this capacitor. In this, it is assumed that the charge generated during an EVC experiment will act like a chemically generated charge, resulting in flow at the wall−solution interface. From the basic physics, it would be expected that the charge created by the EVC in a capacitive system would exist primarily only where the exterior plate exists.[45] Although field lines extend from the edges of the capacitor, the primary and strongest forces will be where the EVC is applied. In this way, it would be expected that either the local ζ potential correction or the weighted average correction should adequately describe the effect of the EVC on the flow rate in the capillary. Yet, neither correction provides a better fit of the experimental data to the models. In addition, work by Hayes, Kheterpal, and Ewing[18] suggests that the EVC is spread evenly over the entire surface, regardless of the amount of coverage on the exterior of the capillary. From this information, it seems reasonable to say that the capillary is not acting as a simple capacitor, and its behavior, while it may be related to a capacitive effect, is not as simple as that described in these models.

Recent work in the Hayes laboratory has also suggested that the EVC effect is not a simple generation of chemical charge on the interior of the capillary.[46] Studies of the effect of EVC on the protein adsorption at the wall in CE were conducted and show that electrostatically generated charge influences protein absorption differently from the same amount of chemically generated charge.

Shah, Wang, and Lee provide additional information regarding this phenomenon.[47] In this work, an organic matrix that contains $Co3^+$ ions is created on the interior of the capillary. The ionic charge is distant from the outer plane of the matrix and is, thus, not a wall effect. However, this charge is seen by the molecules in the capillary, which results in a migration in the direction opposite from a normal CE system. This effect is obviously not a wall effect, and yet, it results in a change in flow rate just as a chemically generated charge would. Clearly, when describing CE, wall effects and charge cannot be dealt with as simplistically as they have been in the past.

From this information, it seems clear that the mechanism of EVC is not a direct capacitance. Some differences exist between the normal flow generation in CE and the new effect from the EVC or matrix components inside the wall. As yet, the specific mechanism is still unknown and requires further investigation.

ACKNOWLEDGMENT

The authors thank the American Chemical Society Petroleum Research Fund (99-0286) and ASU for support of this work.

Received for review July 19, 2001. Accepted November 27, 2001.

AC010816Y

(46) Smith, M. R.; Decker, T. M.; Hayes, M. A. Unpublished results, **2001**.
(47) Shah, R. S.; Wang, Q.; Lee, M. L. In *New Epoxy-Resin Coating for Capillary Electrophoresis*, Proceedings of the 24th International Symposium on Capillary Chromatography and Electrophoresis, Las Vegas, Nevada, 2001.